

Static Live Load Tests on a Cable-Stayed Bridge

J. LEROY HULSEY AND DAVID K. DELANEY

A 91.4-m (300-ft) fracture critical cable-stayed bridge near Skagway, Alaska, carries conventional traffic and 712-kN (160,000-lb) ore trucks. The bridge has a laminated timber deck supported by transverse floor beams spanning two stiffened ASTM A588 steel box girders. Two inclined cables stay each girder near mid-length to a single tower. The abutments and tower are rock-anchored to the canyon walls. The bridge was instrumented and field tested with statically positioned trucks to help determine boundary conditions provided by rock anchor supports and assess behavior for non-AASHTO ore trucks. Two types of trucks were used to load the bridge: (a) a 176.84-kN (39.74-kip) snooper truck, and (b) four different ore trucks with weights from 699.1 to 701.1 kN (155.1 to 157.6 kips). A fracture critical inspection was also conducted and cracks were found. Strain, girder deflection, a temperature profile of the girder, wind velocity, solar radiation, and ambient air temperature were monitored. Experimental deflections and strains compared with a traditional two-dimensional (2-D) analysis are presented. Maximum strains for ore truck static load tests were: 224 microstrain (276 calculated) in the box girder and 134 microstrain (193 calculated) in the tower support. Ore truck loads did not vary significantly and like loading produced excellent repeatability. For this structure, a 2-D analysis provided satisfactory results for symmetric loads; conservative answers on the loaded side for asymmetric loads. A three-dimensional analysis is suggested for modifications. Rock anchors acted as fixed supports.

Consider an unusual 91.44-m (300-ft) cable-stayed highway bridge near Skagway, Alaska. The bridge carries about forty 712-kN (160,000-lb) ore trucks a day in addition to normal traffic and is exposed to harsh climatic conditions. The backstays, tower, and abutments are anchored to the canyon walls with prestressed rock anchors. Recently, modifications were made to provide for an increase in ore truck load limits and volume of traffic (Arvid Grant and Associates, unpublished data). This paper is based on the bridge condition before 1991–1992 design modifications.

GENERAL INFORMATION

The Captain William Moore Creek bridge is a two-lane bridge located between Skagway, Alaska, and Carcross, Canada. A 5.08-cm (2-in.) asphalt wearing surface is attached to a timber deck with wire mesh. The deck consists of 17.78-cm (7-in.) laminated timber planks supported by transverse floor beams spaced at 3.66 m (12 ft) on center. Floor beams connected

by shear plates (no-moment transfer connection) span two stiffened ASTM A588 steel box-shaped girders (Figures 1 and 2). Each girder is supported at the ends by columns and a bearing assembly at the pylon and is stayed about mid-span by cable pairs in a double plane arrangement. The pylon bearing assembly has a curved steel plate adjacent to and slightly below a 2.54-cm (1-in.) neoprene pad. The bridge length of 91.44 m (300 ft) is divided into four span lengths of 9.14, 36.16, 38.17, and 6.10 m (30, 123, 127, and 20 ft) [Figure 1 (*top*)].

The two main box-shaped longitudinal girders are 80 cm (2 ft 6 $\frac{1}{8}$ in.) wide and 154.9 cm (5 ft 1 in.) deep and fabricated from 18.28-m (60-ft) ASTM A588 steel plates welded and spliced at the ends with bolts [Figure 1 (*bottom*)]. Ventilation ports were not installed. Each girder is stayed by two inclined cables 7.62 cm (3 in.) in diameter made of galvanized structural strands that extend through the girders and are anchored to the underside of the bottom flange. The stays are supported above the deck by an inclined H-shaped tower. The tower is supported by the canyon wall and extends up to and supports the girders and then continues approximately 32.31 m (106 ft) with a tapered box-shaped cross section. The ASTM A588 steel tower is inclined forward over the canyon wall at about 15 degrees to vertical. The backstays terminate at tripod supports attached to the canyon by prestressed rock anchors.

The bridge was designed in 1974 (constructed in 1975) for AASHTO HS20-44 highway loads. During winter 1986–1987, cover plates were welded to the main girders to strengthen the bridge to accommodate ore truck traffic between a mine at Whitehorse, Canada, and a barge port in Skagway. Final inspection was completed in February 1987. Between 1986 and 1990, in addition to other traffic, up to 40 ore trucks a day made round trips across the bridge. On each trip to Skagway, a loaded truck weighs about 712 kN (160,000 lb); on the return trip, an empty truck weighs 244.7 kN (55,000 lb).

Sometime during the latter part of 1987, a request was made to increase ore truck load limits to 756.5 kN (170,000 lb) and the trips to 50 per day. Subsequently, the Alaska Department of Transportation and Public Facilities (AKDOT&PF) performed a two-dimensional (2-D) analysis for the existing loading. Calculated stresses were significantly affected by boundary condition assumptions, which led to the question: Do prestressed rock anchor supports act as pinned, fixed, or other? This influenced decision making. Other questions were these: Is a 2-D model sufficient? What type of elements should be used? How are non-AASHTO loads distributed to the girders? Answers were not available by mathematical means.

In 1988 the bridge was instrumented and static-tested with a control load (snooper truck) and four ore trucks. Strains

J. L. Hulsey, Transportation Research Center, University of Alaska Fairbanks, 263 Duckering Building, Fairbanks, Alaska 99775. D. K. Delaney, Centennial Engineering, Inc., 15000 West 64th Avenue, Arvada, Colo. 80004.

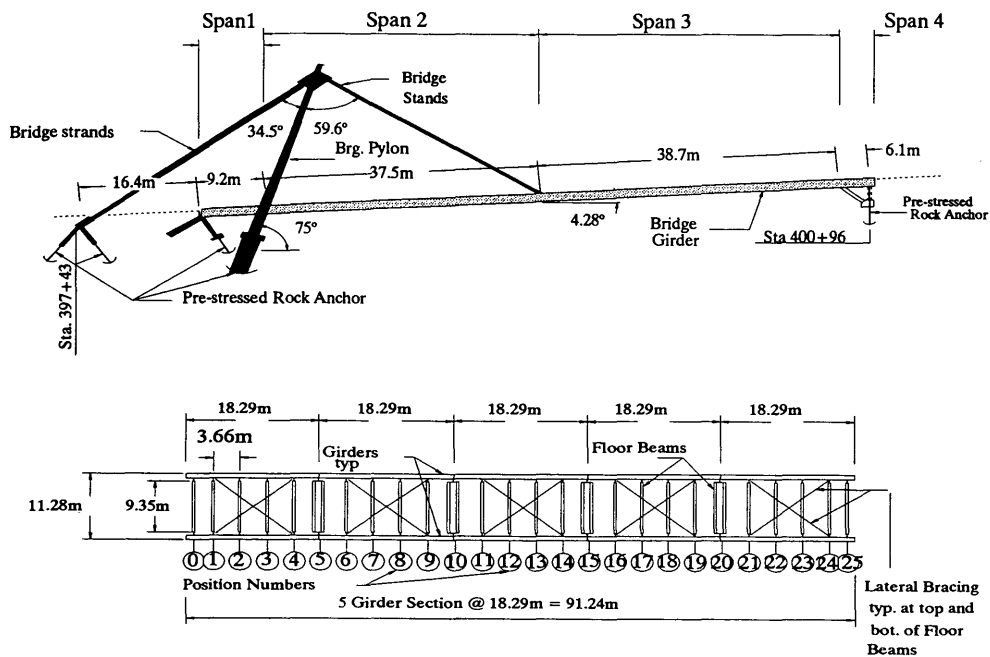


FIGURE 1 Captain William Moore Creek bridge geometry: *top*, bridge geometry elevation; *bottom*, bridge frame plan view.

and girder deflections were recorded to assist in obtaining answers to the preceding questions.

During 1991 and 1992 cracks were found during fracture critical inspections of the bridge (Arvid Grant Associates and Mayes Testing, unpublished data). A three-dimensional (3-D) sophisticated analysis was performed in 1990, dynamic

tests in 1991 and 1992, and structural modifications in 1991 and 1992; these results will be presented later.

It is the purpose of this paper to give static test results for a control vehicle and ore truck loading, show an experimental comparison with a 2-D analysis, and present the general condition of the structure. The validity of using a 2-D model is

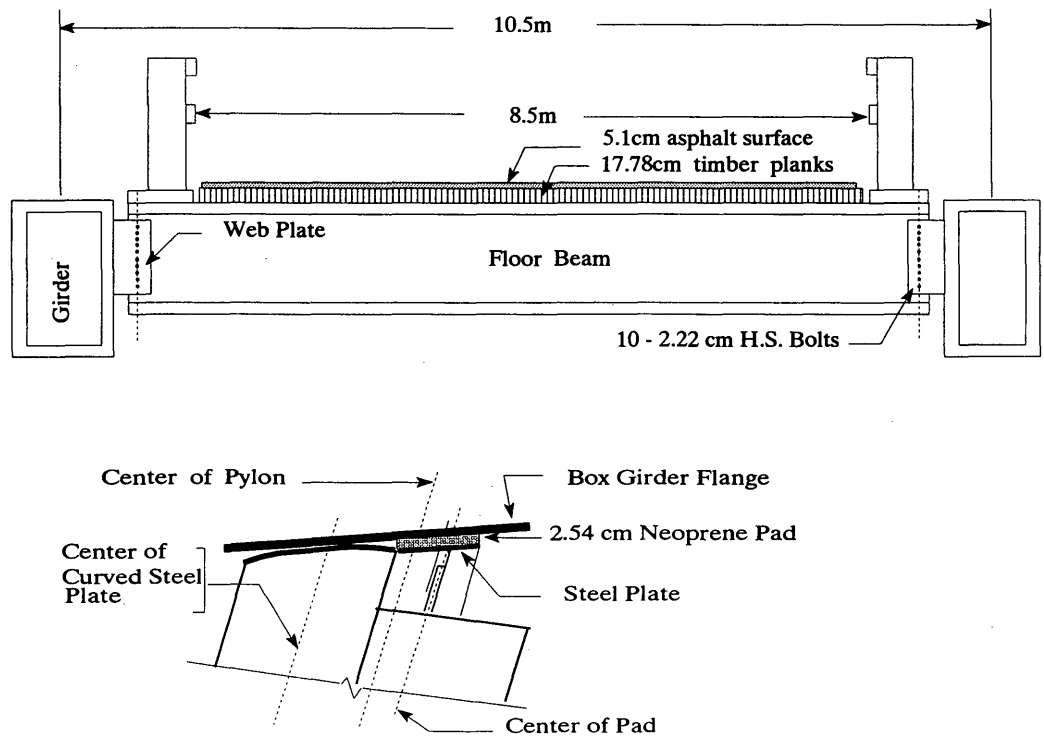


FIGURE 2 Bridge section geometry: *top*, bridge section; *bottom*, pylon bearing pad.

discussed. Degree of fixity for rock anchor supports and sensitivity of the girder pylon bearing assembly are discussed.

STATIC TESTS

The literature reveals that laboratory models of cable-stayed bridges have been used to study erection stresses, construction sequencing, cable anchorage stresses, and nonlinear effects and to develop techniques for analysis and design of these types of structures (1-3).

In the full-scale testing category, the 366-m Tjorn Bridge in Sweden was subjected to dynamic tests 1 week before being opened to traffic (4). Acceleration measurements were taken for three types of tests: dynamic load, free decay, and forced vibration. Except for tests on this structure (5-7), there is no evidence of field static tests on cable-stayed bridges in the literature.

Planning and Preparation

Before an instrumentation strategy was formulated, an analysis was conducted and influence lines were prepared for the

box girders. This information was used to locate strain gauges and position trucks for field testing. Instruments selected were 25 full-bridge, 350-ohm weldable strain gauges; a 25.4-cm (10-in.) clamp-on extensometer; transit and level; velocity seismoprobe; eight 3000-ohm thermistors; one Type-T thermocouple; an annometer; and a pryonometer. Because of a limited budget, rosettes were not used.

Field Test Procedure

Each test was designed to provide results for a known truck load at a given static position on the bridge. This was accomplished by referencing for each test (a) the type of truck, (b) its position across the deck, (c) the location of the front axle along the girder, and (d) the direction of movement (Figure 3). The terms left and right are used to reference truck position across the roadway when facing upstation.

For each test, the front wheels of a truck were positioned in a lane or centerline over paint marks on the deck. Data were collected with a data acquisition system and stored on a floppy disk; the system was located in a van parked off the bridge (Figure 3) (5-7).

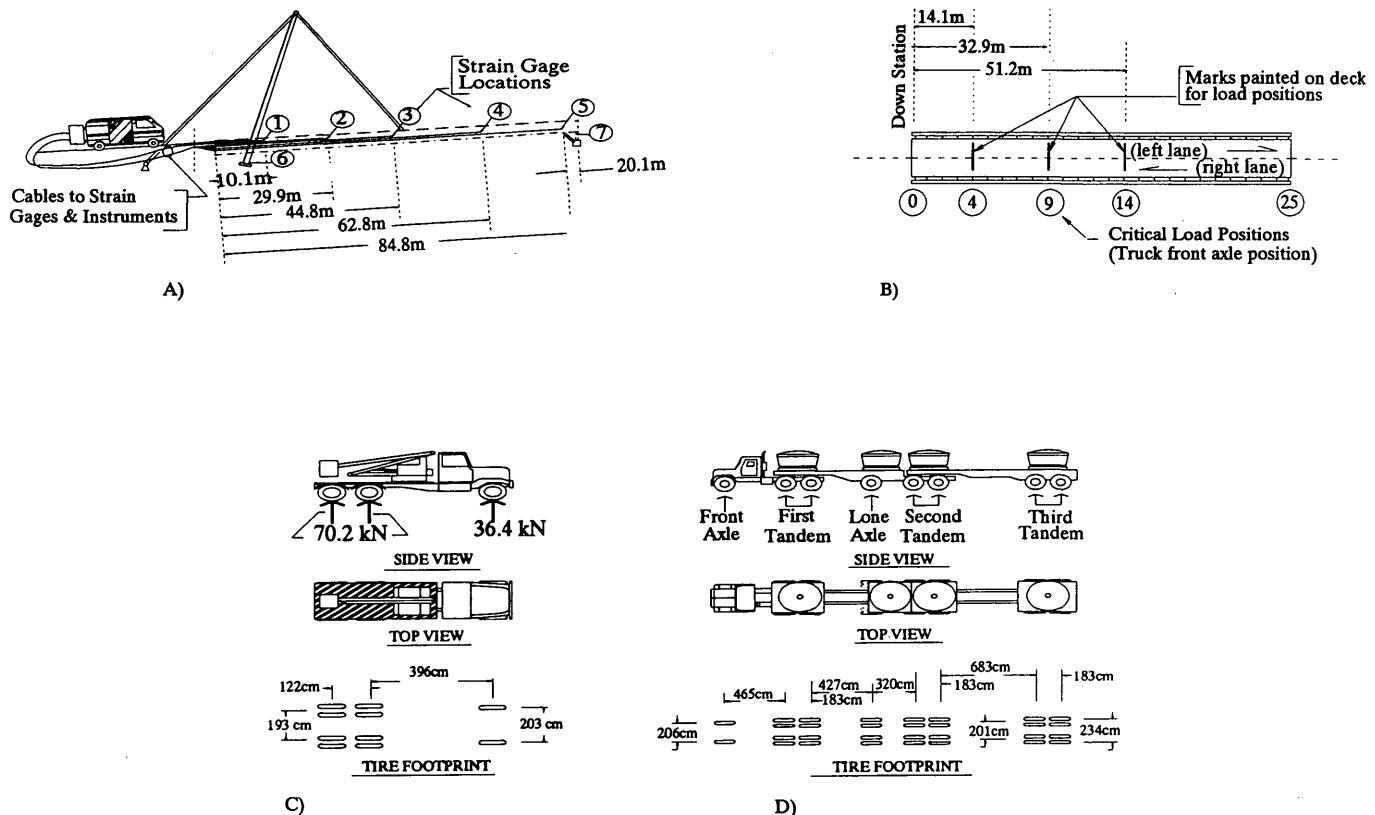


FIGURE 3 Arrangements for testing: a, instrument monitoring equipment; b, bridge frame and load position; c, snooper truck; d, B-train (ore truck).

A typical static test series involved initializing instrumentation, positioning the truck, and checking for vibration dampening with a velocity probe; then time and voltages for each strain gauge, linear variable differential transformer, thermistor, anemometer, and pyranometer were recorded. Vibrations of the structure occurred from normal movements, potholes in the asphalt, and wind.

Field Tests

Two types of trucks were used for static load tests over a 2-day period (Figure 3). The first was a snoopier (control vehicle) approximating AASHTO H20-44 with a front-axle weight of 36.4 kN (8.18 kips) and two axles of 70.22 kN (15.78 kips) each. On the first day, five series of tests for a total of 106 load positions were conducted with the snoopier truck: 53 with the truck in the left lane, 28 in the right lane, and 25 on the centerline (Table 1). Girder elevations were measured for nine of the 106 load positions. Because of procedural errors (electronic spikes from a hand-held radio), data for the first 25 tests were contaminated and rejected.

On the second day, data were recorded for three load positions for four B-trains (Table 1). Each B-train carried ore in four pots mounted on the lowboy trailers (Figure 3d). Truck weights varied from 690.06 to 701.12 kN (155.07 to 157.556 kips). Axle weights for B-trains were obtained from weight tickets. Twelve static B-train tests were conducted: six in the left lane, three on the bridge centerline, and three in the right lane. Girder elevations were measured for 6 of the 12 tests.

TEST RESULTS (EXPERIMENTAL AND ANALYTICAL)

Cable stiffness is dependent on cable tension, angle, weight, and end restraints (8; D. K. Delaney, unpublished data, 1990). Therefore, several techniques have been suggested for analysis of cable-stayed bridges, such as iterative 2-D methods

(9,10), 3-D methods (11-13), and elastic-plastic schemes (14). Others have used models to predict nonlinear behavior (1,3,15). It is one of the objectives of this paper to determine whether a 2-D linear elastic finite element model with beam and axial elements can be used with enough accuracy to calculate strains and deflections.

Finite Element Models

A two-dimensional frame analysis computer program with 6 degrees of freedom (d.o.f.) beam elements, 2 d.o.f. axial elements, linear/axial rotational springs with provisions for eccentric connections, linear flexibility matrix, and nonlinear axial springs were selected. Nodal point loads, concentrated element loads, varying distributed element loads, element temperatures, element strains, and load case combinations are available in the program library.

The program was modified to create a table of computed forces and a table of displacements for the elements and nodes that correspond with measured values. A postprocessor was written in FORTRAN 77 to transform computed forces into strains, sort the information, and create tables comparing computed strains and deflections with experimental results.

Parametric Studies

The analytical study was used to determine the degree of fixity provided by rock anchor supports and the adequacy of a 2-D analysis. In an attempt to seek answers, parametric studies were initiated to investigate boundary condition sensitivity, influence of constant section element approximations of the tapered pylon, and interaction between the curved steel bearing plate and neoprene pad at the pylon bearing assembly. These parameters were studied by comparing analytical with experimental results for load positions when the B-train was on the bridge centerline.

TABLE 1 Truck Test Series

Test	Truck Weights (kN)	Front Axle Positions	Truck		Measured Deflection Locations
			Locations	Movement	
Snooper Truck Test Series:					
SLDOS01	106.86	0-24	Center of left lane	downstation	none
SLDOS02	106.86	0-24	Center of left lane	downstation	none
SLDOS03	106.86	24-0	Center of right lane	upstation	none
SCDOS04	106.86	0-24	Center of bridge	downstation	14,9,4
SCDOS05	106.86	4,9,14	Center of right lane	upstation	4,9,14
		14,9,4	Center of left lane	downstation	14,9,4
B-Train Test Series:					
SLDOB06	690.06	4,9,14	Left lane wheel path	downstation	none
SLDOB08	700.03	4,9,14	Left lane wheel path	downstation	14,9,4
SCDOB10	701.12	4,9,14	Center of bridge	downstation	14,9,4
SRDOB11	699.06	4,9,14	Center of right lane	downstation	none

NOTE: "Left" and "right" refer to view upstation.

Load Distribution

It was assumed that axle weights are distributed equally to each wheel line of the tested vehicles. Each floor beam is connected to a girder with a web plate and a single line of H.S. bolts 2.22 cm ($\frac{7}{8}$ in.) in diameter [Figure 2 (*top*)]. First, it was assumed that the web plate transfers only shear forces (i.e., simple beam theory). The validity of this approximation was tested against both rigid and eccentric shear connector assumptions with girder torsional stiffness included. Analytical comparisons illustrated that simple beam distribution more accurately approximated behavior. Interaction of deck flexibility was not considered.

Pylon and Cables

The upper tapered section of the pylon was approximated with three constant section 6 d.o.f. beam elements. Analysis showed that three equal length elements with section properties for the average section over the length of the element provided satisfactory results. A preliminary investigation of cable tension indicated that sufficient accuracy could be obtained by using linear axial elements (8).

Pylon Bearing Assembly

The box girders are supported at the pylon by a curved steel plate and neoprene pad bearing assembly that is mounted on a shelf [Figure 2 (*bottom*)]. The steel plate was coated with teflon and used to launch the girder and is slightly lower than the neoprene pad. Thus, it was initially assumed that the pad supported the girder. A comparison between analytical and experimental pylon base strains showed that moments were transferred from the girders through both bearings to the pylons; the results further showed that the structure is extremely sensitive to the load path through this bearing assembly. The bearing assembly was approximated by Elements 70, 11, and 68 (Figure 4). Element 70 is a rigid link, Element 11 approximates the plate (large area, zero moment of inertia), and Element 68 approximates the pad (modulus of neoprene, 25 percent pad area since neoprene modulus varies with compressive stress, and zero moment of inertia).

Support Boundary Conditions

Pylons are supported by piles and anchored with prestressed rock anchors (Figure 1). The upstation end bent column is

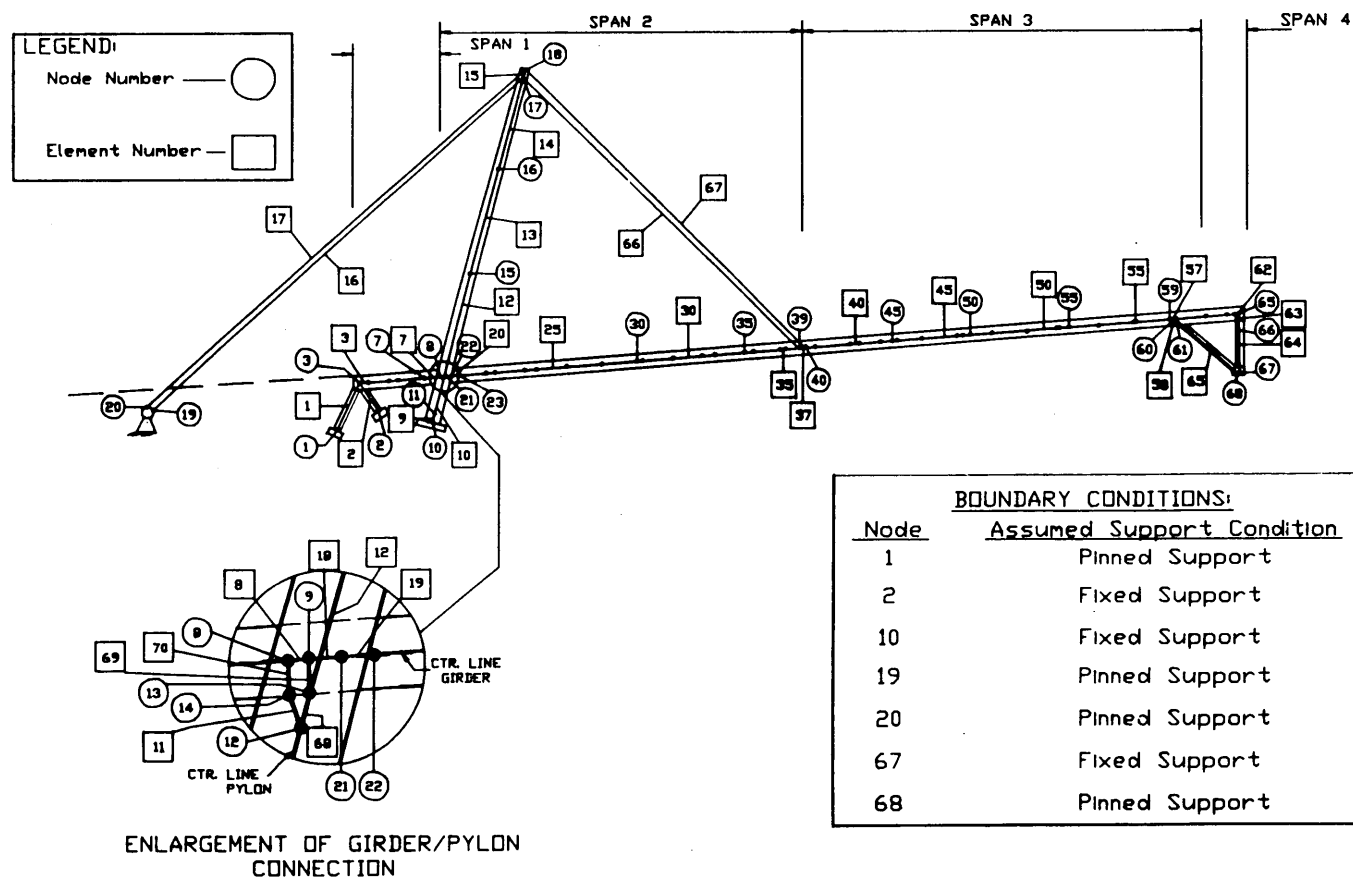


FIGURE 4 Final finite element model.

anchored with prestressed rock anchors, and the base of the strut is not. At the downstation end bent, one is anchored with a prestressed rock anchor and the other is not. Different boundary conditions assumptions were examined by analysis and compared with experimental data. The studies showed that rock anchors act fixed, other supports pinned, and behavior is sensitive to boundary condition assumptions.

Final Model

Except for 2 d.o.f. axial elements used to approximate cables, all members were approximated with 6 d.o.f. beam elements. Nodes were placed at changes in section, floor beam-to-girder connections, locations of strain gauges, pylon intersection, forestay cable connections, and column and strut connections. The final model had 68 nodes, 64 beam type elements, and 4 axial elements (Figure 4).

Strains

Strains at the extreme inside face of the girders, exterior face of the pylon bases (above the stiffeners), and the exterior face of the upstation left column were monitored during testing (Figure 3a). In this paper, results of 9 snoop truck tests and 12 ore truck tests are presented for a truck at positions 4, 9, and 14 for left lane, bridge centerline, and right lane (Table 1). For comparative purposes, the snoop truck weighed 176.85 kN (39.74 kips) and the four ore trucks weighed 690.06, 699.06, 700.34, and 700.3 kN (155.07, 157.093, 157.379, and 157.379 kips).

Figures 5 and 6 show a comparison between measured and calculated girder strains for three truck positions when a 700.3-kN (157.379-kip) B-train is parked in the left lane. The results show that calculated strains overpredict strains for the left girder and underpredict the right girder. Figure 7 shows that except for a change of section near the strut (84.8m), calcu-

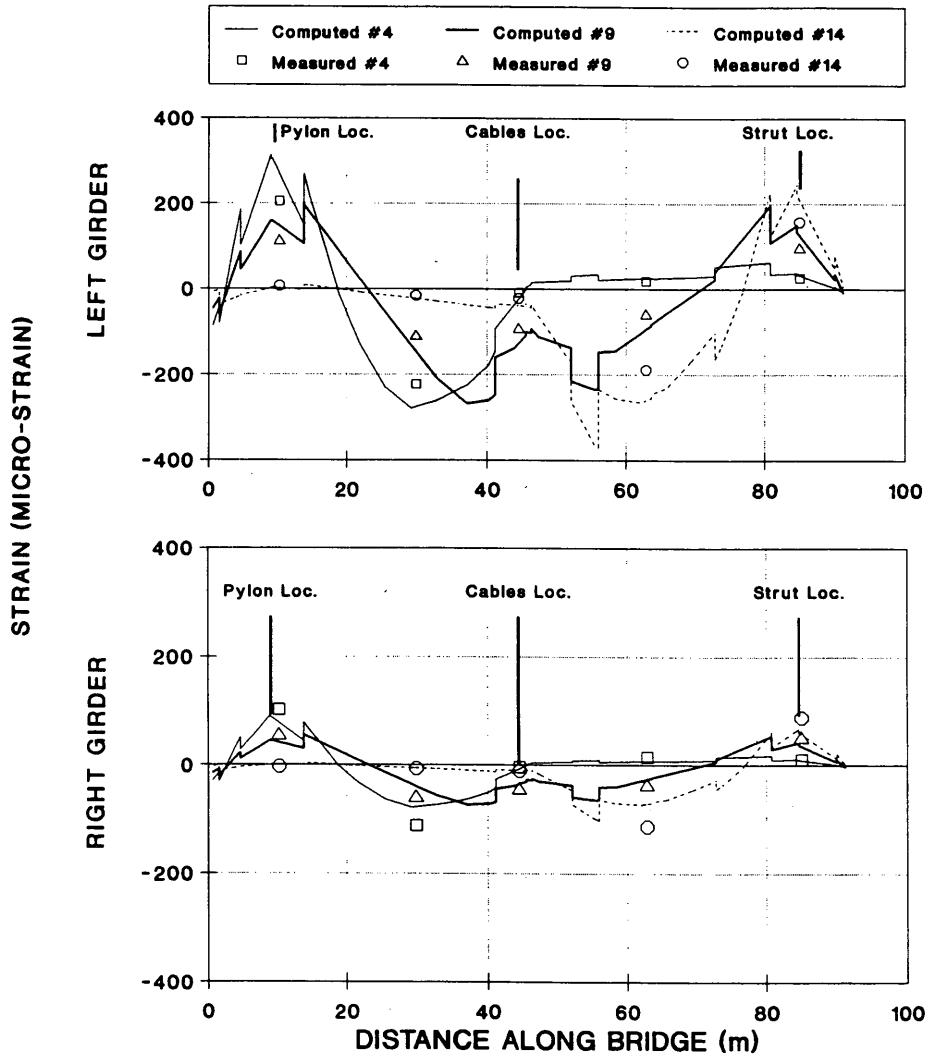


FIGURE 5 Top of girder strains, 700.3-kN (157.379-kip) B-train in left lane.

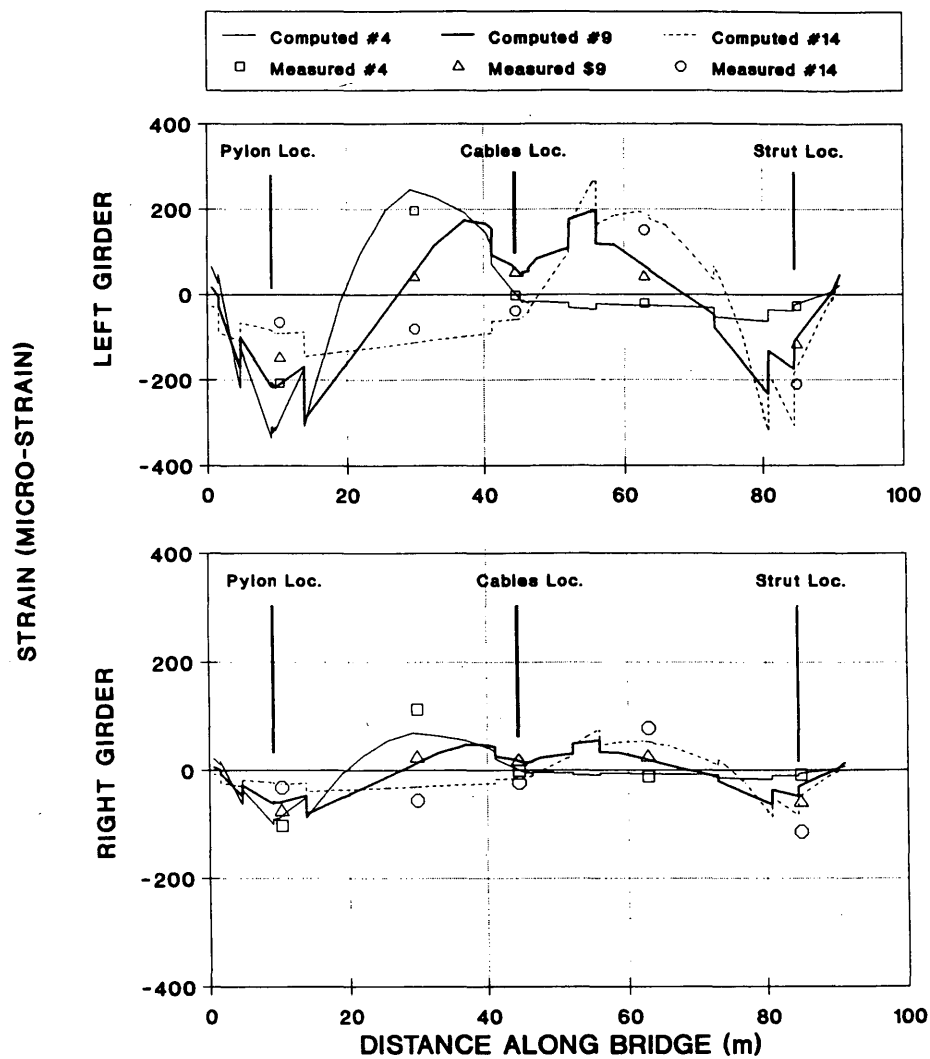


FIGURE 6 Bottom of girder strains, 700.3-kN (157.379-kip) B-train in left lane.

lated and experimental strains compare well when a 701.1-kN (157.556-kip) B-train is parked at three positions on the bridge centerline. Figure 8 shows that the calculated top of girder strains overpredict experimental strains on the loaded side and underpredict on the unloaded side when a 699.1-kN (157.093-kip) B-train is parked in the right lane. Similar results were found for the bottom of the girder.

Table 2 presents a comparison between measured and calculated girder strains for the three B-train static tests. The results show that the maximum measured girder strain is 224 microstrain and the corresponding calculated value is 276 microstrain.

Table 3 gives maximum measured strains in girders, pylon, and upstation columns for the three B-trains. Except for a condition when the truck was on the bridge centerline, calculated maximum strains typically overpredicted the maximum experimental strains.

For comparison, a summary of 9 snooper truck tests and 12 ore trucks at the three load positions is presented in Table 4.

Girder Deflections

Fog and wind precluded accurate deflection data for most of the snooper truck tests. However, the maximum measured snooper truck girder deflection for load positions 4, 9, and 14 was 1.96 cm (0.77 in.). The maximum girder deflection for the B-train tests occurred in position 9, with a truck in the left lane giving 7.0 cm (2.76 in.) measured and 8.6 cm (3.4 in.) calculated. The maximum girder deflection for a B-train on the bridge centerline was 5.49 cm (2.16 in.) measured and 5.54 cm (2.18 in.) calculated. Figures 9 and 10 present calculated and experimental deflections for B-train loads. The deflections show that the analysis overpredicts the loaded side

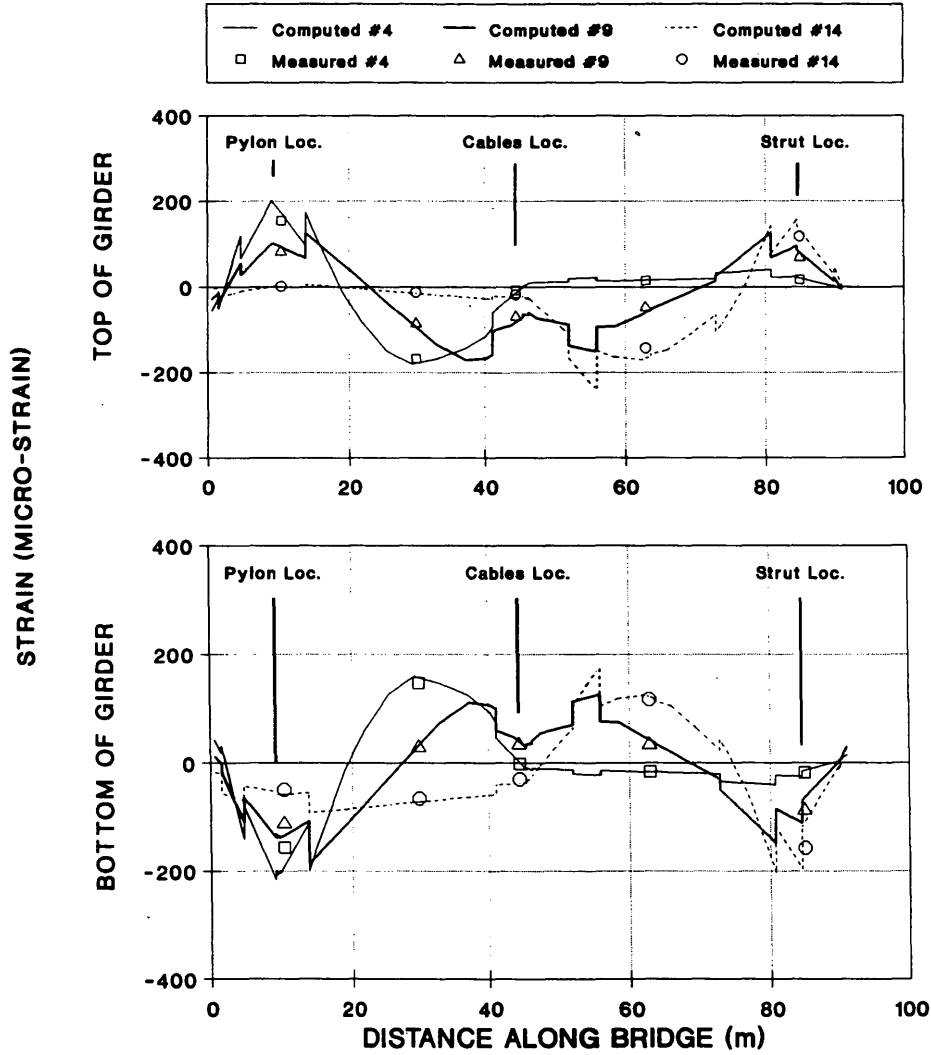


FIGURE 7 Girder strains for 701.1-kN (157.556-kip) B-train on centerline.

for asymmetric loading and gives accurate results for symmetric loading.

FRACTURE CRITICAL INSPECTION

An inspection of the cable-stay assemblies was conducted in September 1990 (Arvid Grant and Associates, unpublished data) using ultrasonic, magnetic particle, and X-ray nondestructive testing. Cables, zinc-poured cable anchorage sockets, and cable anchorage connections were inspected. Cables, spanner nuts, and connectors were in good condition. An X-ray of the anchorage sockets revealed cracks in the zinc and voids between the zinc, cable wires, and steel socket. In June and July 1991, visual and magnetic particle inspections were performed on the upper pylon and strand connection plate welds, box girder cover plates, box girder internal longitudinal stiffeners, and floor beam connections (Mayes Testing Engineers, unpublished data). Fifty percent of the cover plate ends (14) showed signs of cracks (Figure 11). Most of the cracks were in the ASTM A588 girder flanges

adjacent to the fillet weld toe, in or near the zone affected by the weld heat. Approximately 80 weld terminations were examined inside a box at the longitudinal stiffeners, with no cracks found. Cracks were visually evident at the top of the floor beam webs at the termination of the web flange weld in 31 of 60 locations and 1 bottom location. The largest cracks in the beam webs exceeded 2.54 cm (1 in.). The floor beam webs were not coped. Other items found included three deep gouges in the flange of one box girder and improper welding techniques. In June 1992, fracture critical inspections were again conducted to assess crack growth. Ten of 18 previously cracked locations showed some crack growth.

SUMMARY AND CONCLUSIONS

Experimental results indicated that wheel loads on the loaded ore trucks did not vary significantly and, like loading produced excellent repeatability. Comparisons between analytical and

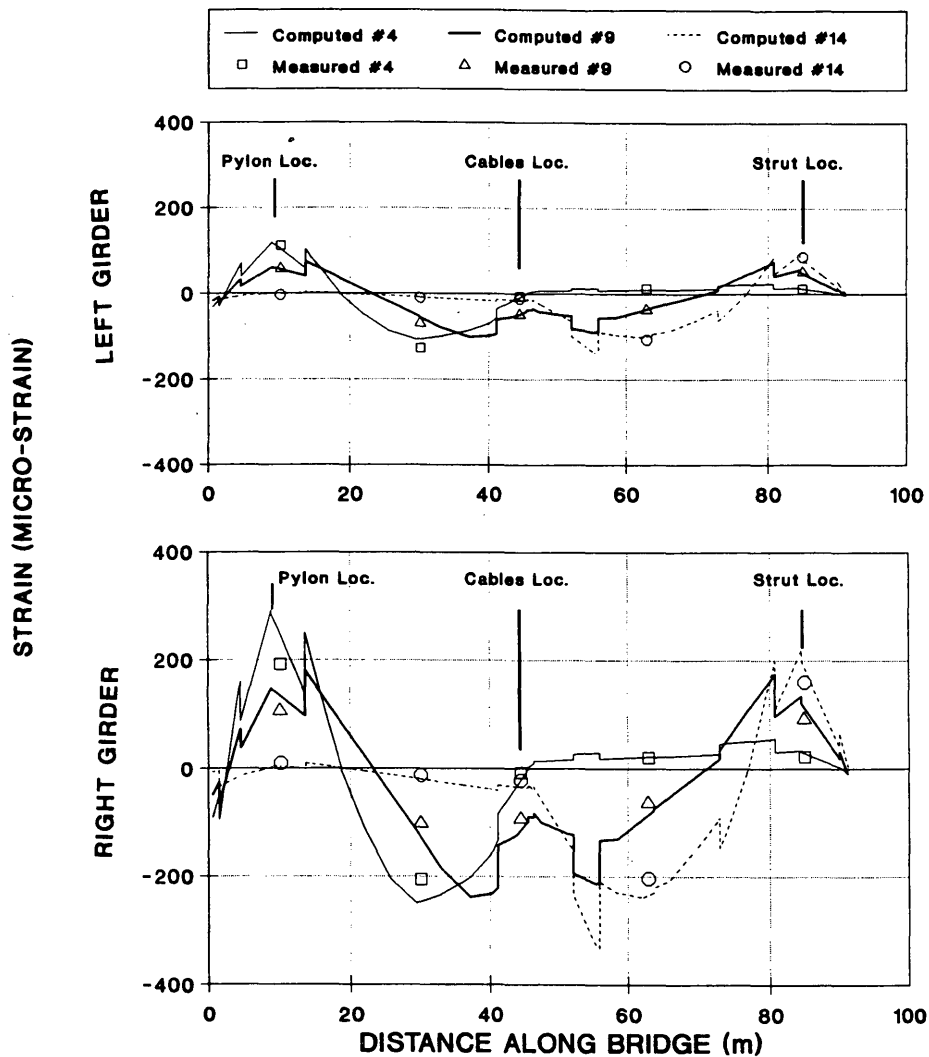


FIGURE 8 Top of girder strains, 699.1-kN (157.093-kip) B-train in right lane.

experimental results showed that

- Behavior is sensitive to interaction between the curved steel plate and neoprene bearing pad at the girder pylon interface (i.e., results were influenced by deformation of the neoprene);
- Boundary condition assumptions significantly influenced load distribution; and
- Supports with prestressed rock anchors act fixed and other supports act pinned.

A 2-D linear elastic model was satisfactory for symmetrically applied loads. For asymmetrical loads, the 2-D model overpredicts the load side and underpredicts the unloaded side of the structure. A 2-D model (conventional frame programs) will give conservative answers for this geometric configuration as long as special attention is given to the support conditions.

Floor beams were connected to the box girders with shear connections. At this connection, the web-to-flange of the floor

beam was not properly coped and visible cracks existed at the top of the web in more than 50 percent of the floor beams. In 1987 cover plates were added to the flanges of the ASTM A588 box girders to accommodate 712 kN ore truck loads. In 1991 and 1992 about 50 percent (14 locations) of the flanges in this fracture critical structure showed evidence of cracks at the weld terminations at the end of the cover plates. Generally, the cracks varied between 0.16 to 3.12 cm and were approximately 0.16 cm deep.

Calculated maximum stresses using a 2-D model were conservative. However, because of cracks and a need to strengthen the structure for heavier loads and more traffic, this structure should be tuned for asymmetric loads by a 3-D model with provisions for geometric nonlinear stiffness of existing or additional cables. It is important that the material condition of fracture critical structures be considered when modifications are made. Visible cracks are difficult to identify in ASTM A588 steel, and nondestructive testing should be used at critical locations.

TABLE 2 Strain Extremes for Symmetric and Asymmetric B-Train Loads

Gauge Loc. (m) a)	Top of Girder (microstrain)								Bottom of Girder (microstrain)							
	Left Girder				Right Girder				Left Girder				Right Girder			
	Max. Tens.		Max. Comp.		Max. Tens.		Max. Comp.		Max. Tens.		Max. Comp.		Max. Tens.		Max. Comp.	
	Exp	Calc	Exp	Calc	Exp	Calc	Exp	Calc	Exp	Calc	Exp	Calc	Exp	Calc	Exp	Calc
Symmetric																
10.1	153	175	---	---	152	178	---	---	---	---	157	191	---	---	158	193
29.9	---	---	169	178	---	---	164	176	146	157	67	72	163	156	74	72
44.5	---	---	69	82	---	---	72	82	34	40	31	38	33	41	31	47
62.8	14	16	144	167	15	16	165	168	116	122	17	17	111	124	15	15
84.8	117	134	---	---	127	135	---	---	---	---	158	111	---	---	171	111
Max diff. ^b	-22		-23		-26		-12		-11		47		-13		60	
Asymmetric																
10.1	204	272	4	---	191	249	4	---	---	---	208	297	---	---	197	271
29.9	---	---	224	276	---	---	207	216	196	243	81	112	205	219	85	100
44.5	---	---	94	128	---	---	93	115	51	62	38	59	47	56	35	52
62.8	17	25	189	260	20	22	204	234	150	190	22	26	138	173	18	22
84.8	157	210	---	---	160	189	---	---	---	---	211	174	---	---	215	155
Max diff. ^b	-68		-7		-58		-30		-47		-89		-35		-74	

a) 1 m = 3.2787 ft

b) Maximum strain difference = (Measured - Computed)

TABLE 3 Maximum Strains Produced by B-Trains

Load Condition	Truck wt (kN)	Type of Member	Strain (micro-strain)			
			Tension		Compression	
			Exper.	Calc.	Exper.	Calc
A) MAXIMUM B-TRAIN LOAD CONDITIONS						
Symmetrical	699.1-701.1	Along the girders	163	156	171	111
		Pylon base	40	50	99	124
		Upstation column (left side)	22	15	---	
Asymmetrical	699.1-701.1	Along the girders	205	219	224	276
		Pylon base	54	78	134	193
		Upstation column (left side)	26	23	---	
B) B-TRAIN LOAD LOCATION (LANE POSITION)						
Left lane	700.3	Girder (10.1m,29.9m)	204	272	224	276
		Pylon base (left)	54	78	134	193
		Left column	25	23	---	---
Centerline	701.1	Girder (10.1m,84.8m)	163	156	171	111
		Pylon base (left)	40	50	99	124
		Left column	22	15	---	---
Right lane	699.1	Girder (29.9m,29.9m)	205	219	207	246
		Pylon base (right)	26	42	103	143
		Left column	17	9	---	---

1 kN = 0.2247 kips; 1 m = 3.2787 ft

TABLE 4 Bridge Maximum Measured Strains and Stresses

		Experimental		Calculated	
Item	Location	Strain (microstrain)	Stress ^b (kPa)	Strain (microstrain)	Stress ^b (kPa)
Snooper truck					
Left girder	10.1 m ^a	58	11,589	71	14,186
Right girder	10.1 m ^a	53	10,590	72	14,386
Left column	upstation	8	1,598	2	400
Left pylon	base	39	7,792	49	9,791
Right pylon	base	30	5,994	25	4,995
B-train					
Left girder	29.9 m ^a	224	44,757	276	55,148
Right girder	29.9 m ^a	207	41,361	246	49,153
Left column	upstation	26	5,195	23	4,596
Left pylon	base	134	26,774	193	38,563
Right pylon	base	103	20,580	143	28,573

^aDistances are along bridge incline from downstation end; 1 m = 3.279 ft.

^bStress is calculated from $\sigma = E\epsilon$; 1 kPa = 0.1451 psi.

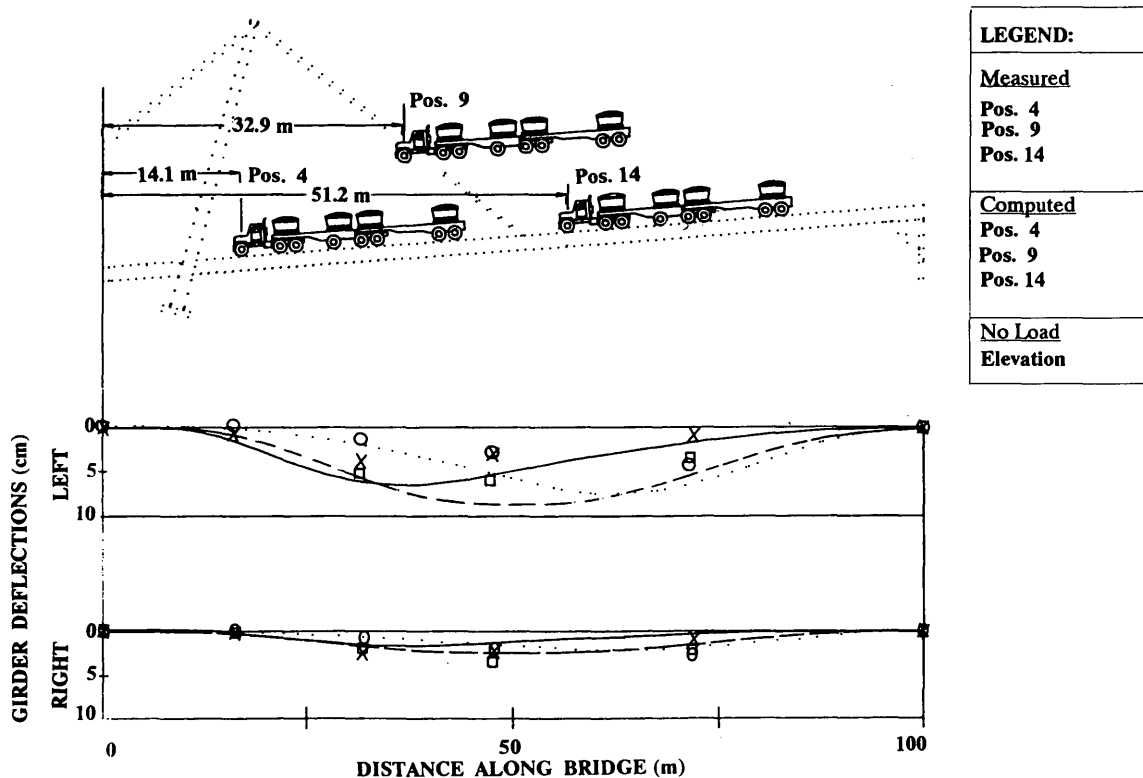


FIGURE 9 Girder deflections, 700.3-kN (157.379-kip) B-train in left lane.

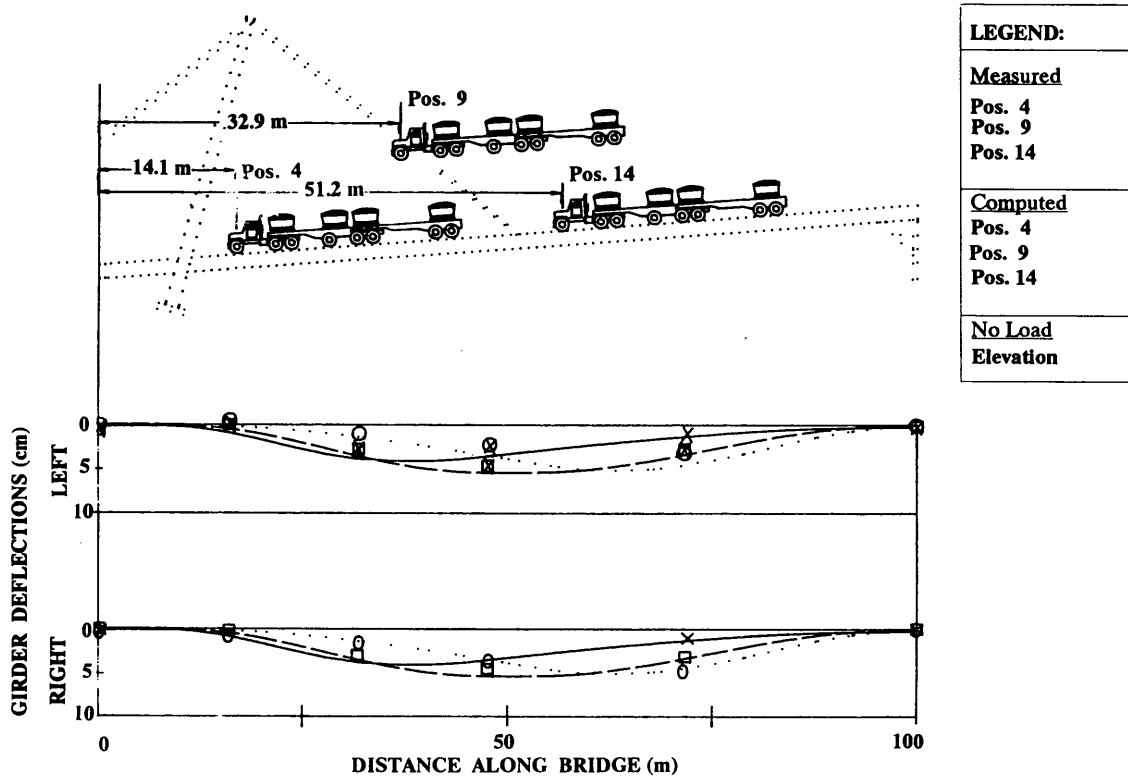
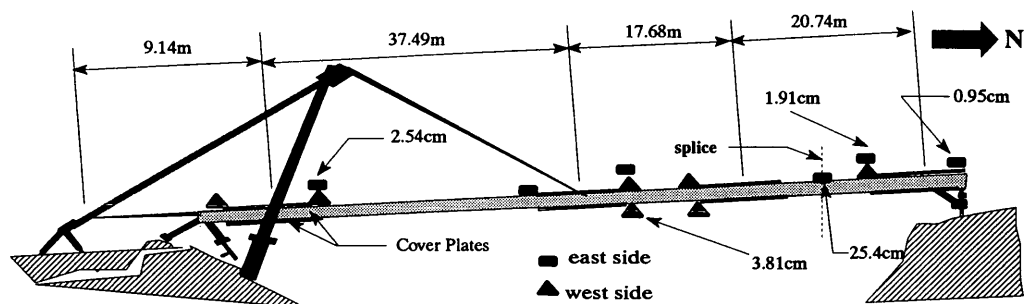


FIGURE 10 Girder deflections, 699.1-kN (157.093-kip) B-train on centerline.



Note: All other cracks are 0.32cm to 0.64cm long

A)

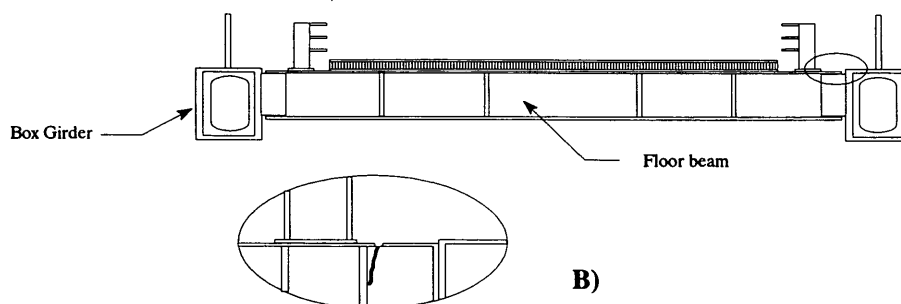


FIGURE 11 Bridge cracks from fracture critical inspections: *top*, crack length at cover plates; *bottom*, cracks at connection.

ACKNOWLEDGMENTS

The authors are grateful for financial support from AKDOT&PF in cooperation with the FHWA. The writers thank Richard W. Briggs, of AKDOT&PF; Rufus B. Bunch, a graduate student who assisted with instrumentation and testing; and Randy Muth, who assisted with the artwork. The writers also acknowledge the University of Alaska, Fairbanks, and the contributions of Arvid Grant and Associates and Mayes Testing Engineers.

REFERENCES

1. T. H. Kayser and J. Binkorst. *Computer Calculations of a Complex Steel Bridge Verified by Model Investigations (Applied at the Steel Bridge Spanning the River Waal Near Ewijk)*. Ministry of Transport, Netherlands, Rijkswaterstaat, The Hague, 1975.
2. M. Koizumi, A. Senpaku, H. Araki, Y. Kosugi, R. Yonehara, and S. Kawanobe. *Construction of Mieko-Hishi Bridge*. Technical Report Overseas 45. Nippon Kokan, Dec. 1985, pp. 2–12.
3. M. S. Troitsky and B. E. Lazar. Model Analysis and Design of Cable-Stayed Bridges. *Proc., Institute of Civil Engineers*, Vol. 48, London, England, March 1971, pp. 439–464.
4. S. Ohleson. *Dynamic Properties of the Tjorn Bridge Experimental Program*. Report 81:3. Chalmers University of Technology, Sweden Institute of Transportation, Onsternik, Staal-och Traebvbggnad. Nov. 1981.
5. J. L. Hulsey, D. K. Delaney, and R. W. Briggs. *Cable-Stayed Static Tests—An Experimental Study for the Captain William Moore Creek Bridge*. FHWA Final Report AK-RD-90-08. Alaska Department of Transportation, Fairbanks, 1989.
6. J. L. Hulsey and D. K. Delaney. *Cable-Stayed Static Linear Analysis for the Captain William Moore Creek Bridge*. FHWA Final Report AK-RRD-90-08A. Alaska Department of Transportation, Fairbanks, 1989.
7. J. L. Hulsey, D. K. Delaney, R. B. Bunch, and R. W. Briggs. *Proc., Eight Structures Congress*, ASCE, Baltimore, Md., 1990.
8. M. S. Troitsky. *Cable-Stayed Bridges; An Approach to Modern Bridge Design*. Van Nostrand Reinhold Company, New York, N.Y., 1988.
9. B. E. Lazar. Stiffness Analysis of Cable-Stayed Bridges. *Journal of the Structural Division*, ASCE, Vol. 98, No. ST7, 1972, pp. 1605–1612.
10. A. M. C. Tang. Analysis of Cable-Stayed Bridges. *Journal of the Structural Division*, ASCE, Vol. 97, No. ST5, 1971, pp. 1481–1485.
11. M. Como, A. Grimaldi, and F. Maceri. Static Behavior of Long-Span Cable-Stayed Bridges. *International Journal Solids and Structures*, Vol. 21, No. 8, 1985, pp. 831–850.
12. Y. C. Loo and S. Srivanich. A Simplified Analysis of Cable-Stayed Box Bridges. *International Journal of Structures*, Vol. 3, Paper 35, 1983, pp. 93–103.
13. C. Crawford and P. Loris. Brooklyn Bridge Computer Model. *Proc., 3rd Conference on Computing in Civil Engineering*, ASCE, New York, N.Y., 1984, pp. 540–549.
14. H. Naki, T. Kitada, R. Ohminami, and T. Nishimura. Elastoplastic and Finite Displacement Analysis of Cable-Stayed Bridges. In *Memoirs of the Faculty of Engineering*, Vol. 26, Osaka City University, Japan, 1985, pp. 251–271.
15. H. Gimsing. Multi-Span Cable-Stayed Girder Bridges. *Journal of the Structural Division*, ASCE, Vol. 102, No. ST10, 1976, pp. 1989–2003.

Publication of this paper sponsored by Committee on Dynamics and Field Testing of Bridges.